Simulations of plasma penetrating magnetic barriers

Herbert Gunell[a], Tomas Hurtig[b], Mark Koepke[a], Nils Brenning[c], and Hans Nilsson[d]

[a] West Virginia University, Morgantown, WV, USA
[b] Swedish Defence Research Agency, Stockholm, Sweden
[c] Royal Institute of Technology, Stockholm, Sweden
[d] Swedish Institute of Space Physics, Kiruna, Sweden

WestVirginiaUniversity

Abstract

Plasma structures, here typified by the term “plasmoids”, in the solar wind impacting on the magnetopause, i.e., the boundary between the solar wind and the earth’s magnetosphere, can penetrate this boundary and be injected into the magnetosphere. This can happen either by expulsion of the magnetic field from the structure and subsequent diffusion of the magnetic field into the structure, or by formation of a polarisation electric field that lets the plasmoid $\vec{E}\times\vec{B}$-drift in the earth’s magnetic field. In both cases a collisionless resistivity is required at some stage of the process. While magnetic expulsion requires electromagnetic models for its description, polarisation can be modelled electrostatically. Both processes can be studied in laboratory experiments.

We present three-dimensional electrostatic particle-in-cell simulations that reproduce large-amplitude waves, in the lower-hybrid range, that have been observed in laboratory experiments. We consider the implications for spacecraft-based studies of magnetopause penetration, and suggest that the search for penetrating plasma structures should emphasise cases in which the interplanetary magnetic field is oriented northward, as this configuration is less likely for reconnection. The application of theoretical predictions to the magnetopause environment shows that a plasma structure penetrating via polarisation needs to be small, i.e., less than 10–100 km wide for typical parameters, and that wave processes at the magnetopause are needed to create such small structures [1]. A larger structure can penetrate by means of magnetic expulsion.

Recent experiments

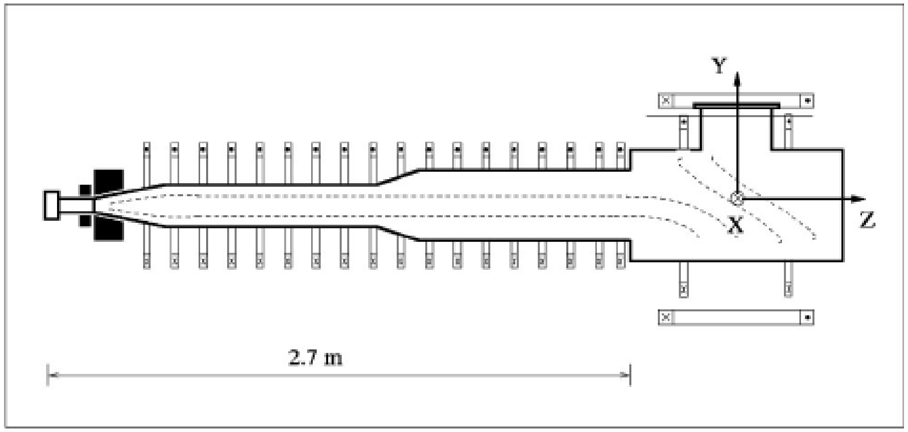

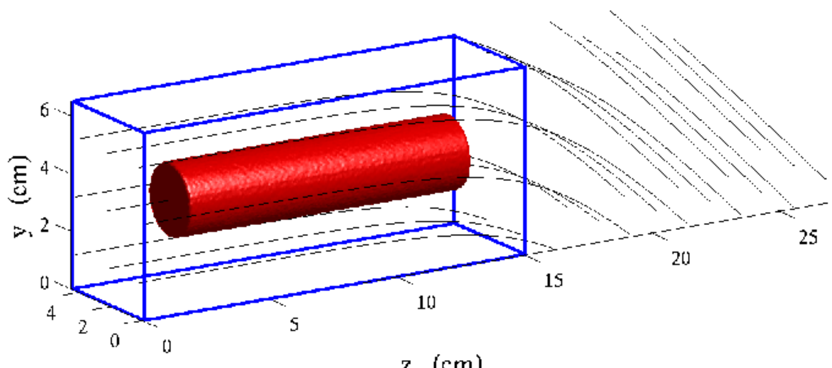

Schematic of the KTH plasma gun; now at WVU (top) [2], and simulation region and magnetic field lines (bottom). The simulation box moves to the right in the figure with the initial bulk velocity of the plasma, v_0.

parameter	sim. I	sim. II	exp. [2]
v_0/(km/s)	300	300	300
$B_\perp$/T	0.05	0.05	0.015
n_0/m^{-3}	10^{15}	10^{16}	10^{18}
m_i/m_e	92	92	1836
W_K/W_E	76	756	$8 \cdot 10^5$
$\frac{1}{10}\frac{W_K}{W_E}\sqrt{\frac{m_e}{m_i}}$	0.79	7.9	$2 \cdot 10^3$
W_K/W_B	$8 \cdot 10^{-5}$	$8 \cdot 10^{-4}$	0.8

$$W_K = \frac{1}{2} n_0 m_i v_0^2$$

$$W_E = \frac{1}{2}\epsilon_0 \left(v_0 B_\perp\right)^2$$

$$W_B = \frac{B_\perp^2}{2\mu_0}$$

Previous results

- When $W_K \gg W_E$ an electric field is set up that allows the plasma to $\vec{E} \times \vec{B}$-drift into the transverse magnetic field [3].
- For quasi-neutrality to be maintained one needs to require that $W_K/W_E \gg \sqrt{m_i/m_e}$ [4].
- It was found experimentally that unless $W_K/W_E > 10\sqrt{m_i/m_e}$ longitudinal oscillations and sheath formation prevent penetration [5].
- A recent series of experiments revealed a wave-driven electron transport, perpendicular to $\vec{B}$ and $\vec{v}_0$, into the high potential side [6].

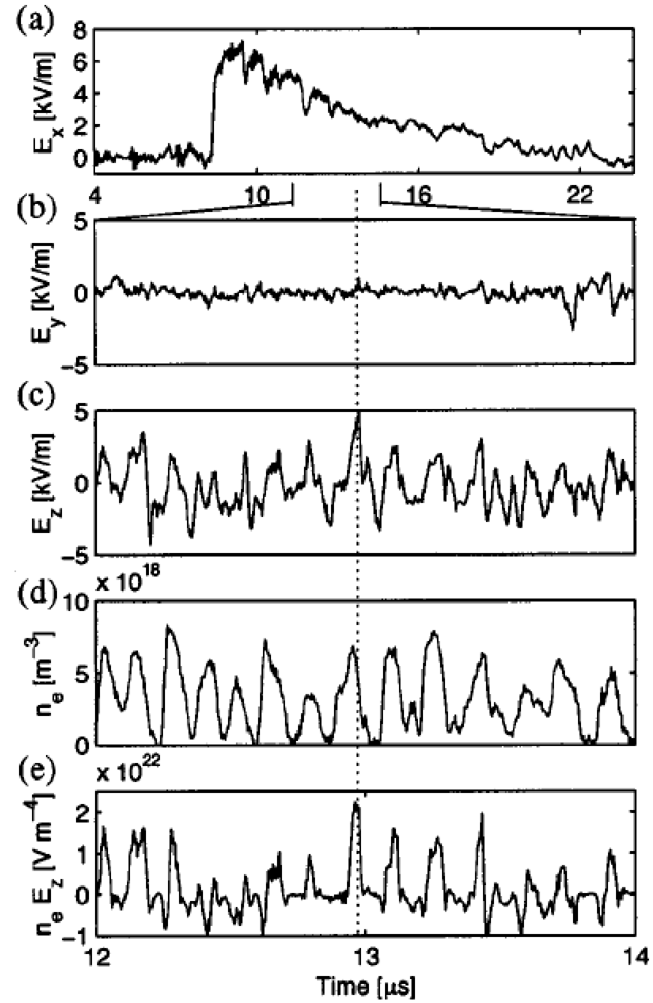

Wave-driven electron drift observed in a plasma gun experiment. Picture from [6].

Parameter regions

Brenning, et al. [7] suggested an analytical model for the non-linear magnetic diffusion, and proposed that experiments and observations can be classified by dividing the parameter space into three regions corresponding to three different outcomes of a penetration experiment. With the width of the plasma equal to w, the ion gyro radius $r_{\mathrm{gi}} = m_{\mathrm{i}} v_0 / (\mathrm{e} B_{\perp})$, the magnetic energy density $W_B = B_{\perp}^2 / (2\mu_0)$, the kinetic beta $\beta_{\mathrm{k}} = W_K / W_B$, the ion thermal beta $\beta_{\mathrm{ith}} = \frac{1}{2} n_0 m_{\mathrm{i}} v_{\mathrm{ith}}^2 / W_B$, and $K = 2.3$ being an empirically determined constant, these regions are [7]

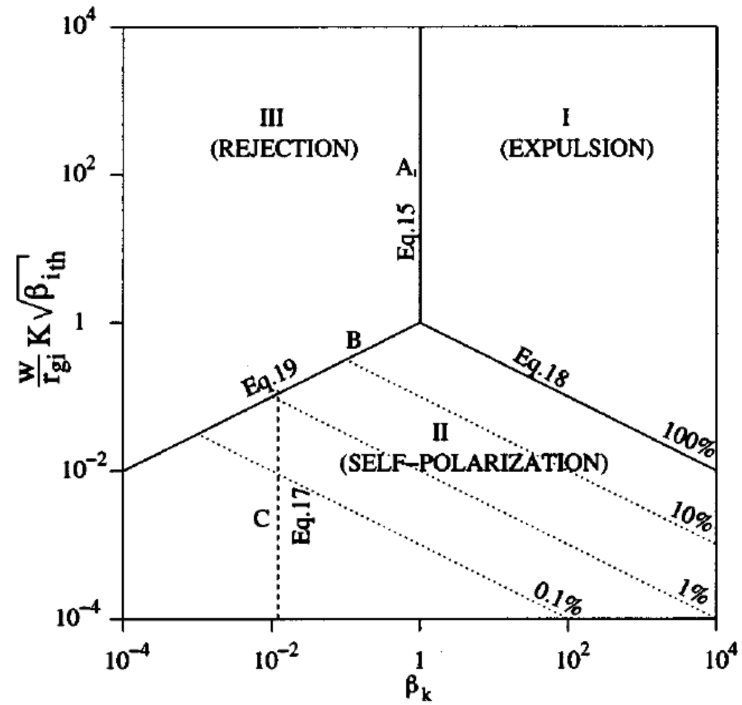

1. **Expulsion.** A plasma structure can penetrate a magnetic barrier by expelling the magnetic field if $\beta_{\mathrm{k}} > 1$ and $(w/r_{\mathrm{gi}})\, K \sqrt{\beta_{\mathrm{ith}}} > 1/\sqrt{\beta_{\mathrm{k}}}$.
2. **Self-polarisation.** A plasma structure can penetrate a magnetic barrier by convection in a polarisation electric field if $(w/r_{\mathrm{gi}})\, K \sqrt{\beta_{\mathrm{ith}}} < \sqrt{\beta_{\mathrm{k}}}$ for $\beta_{\mathrm{k}} < 1$ and $(w/r_{\mathrm{gi}})\, K \sqrt{\beta_{\mathrm{ith}}} < 1/\sqrt{\beta_{\mathrm{k}}}$ for $\beta_{\mathrm{k}} > 1$.
3. **Rejection.** The plasma cannot penetrate the magnetic barrier if $\beta_{\mathrm{k}} < 1$ and $(w/r_{\mathrm{gi}})\, K \sqrt{\beta_{\mathrm{ith}}} > \sqrt{\beta_{\mathrm{k}}}$.

Simulation I

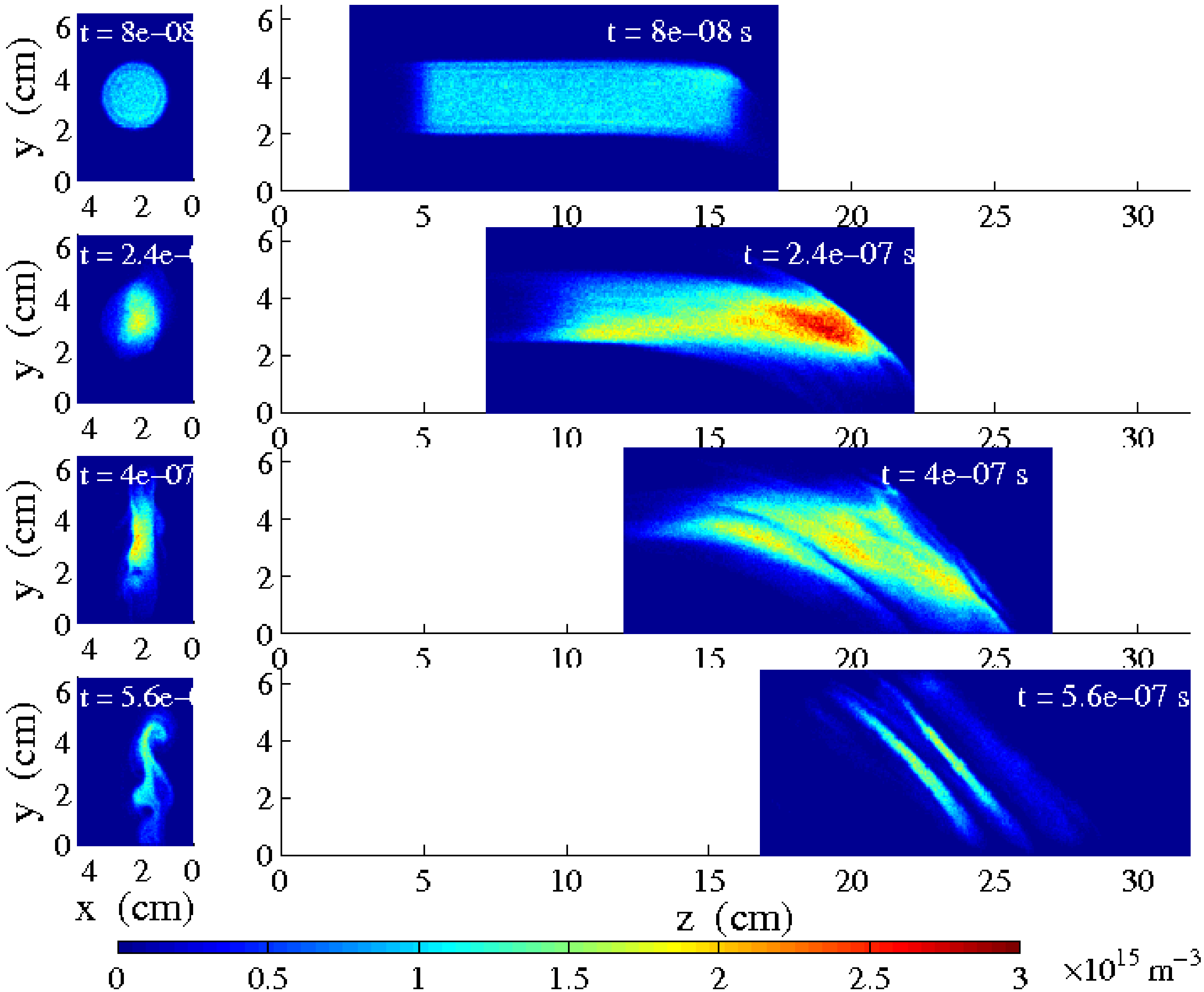

Electron density maps at different times.

Simulation I

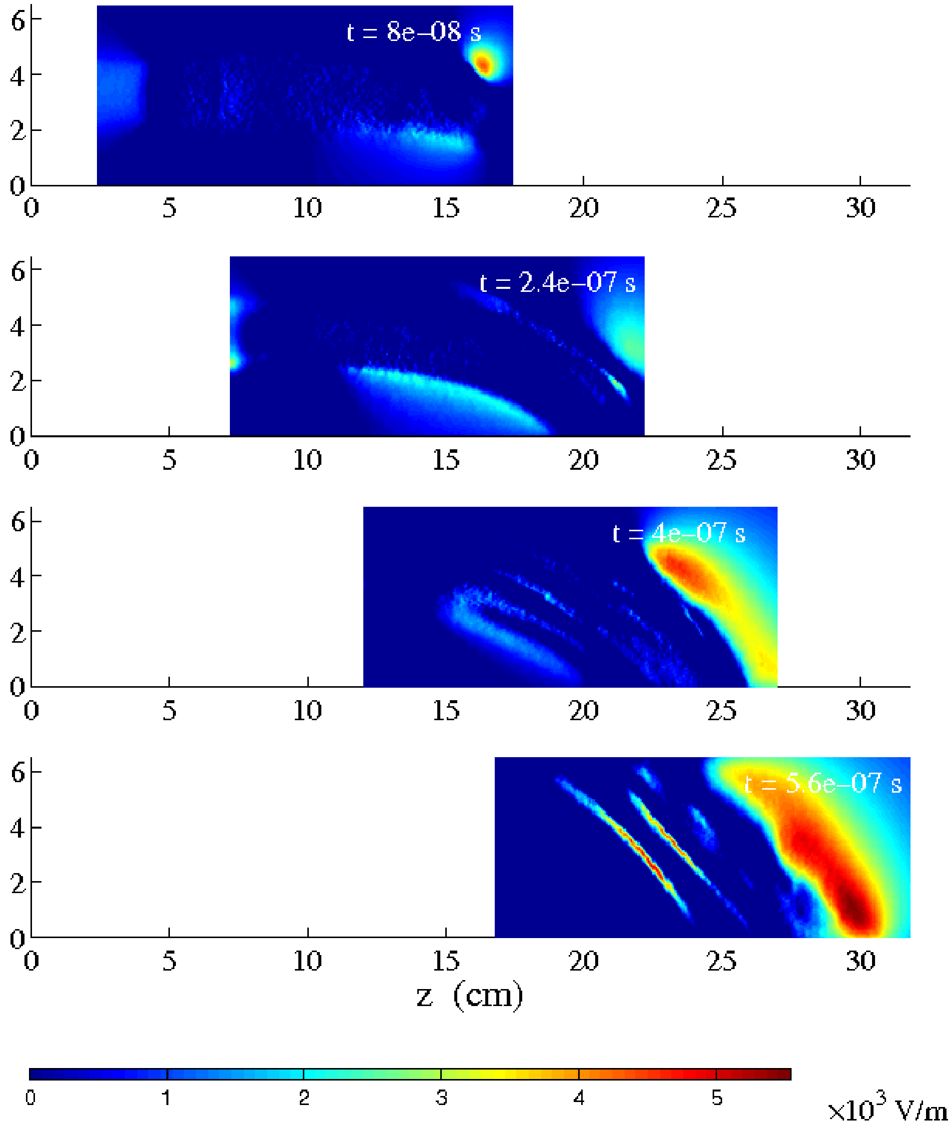

E_z maps at different times.

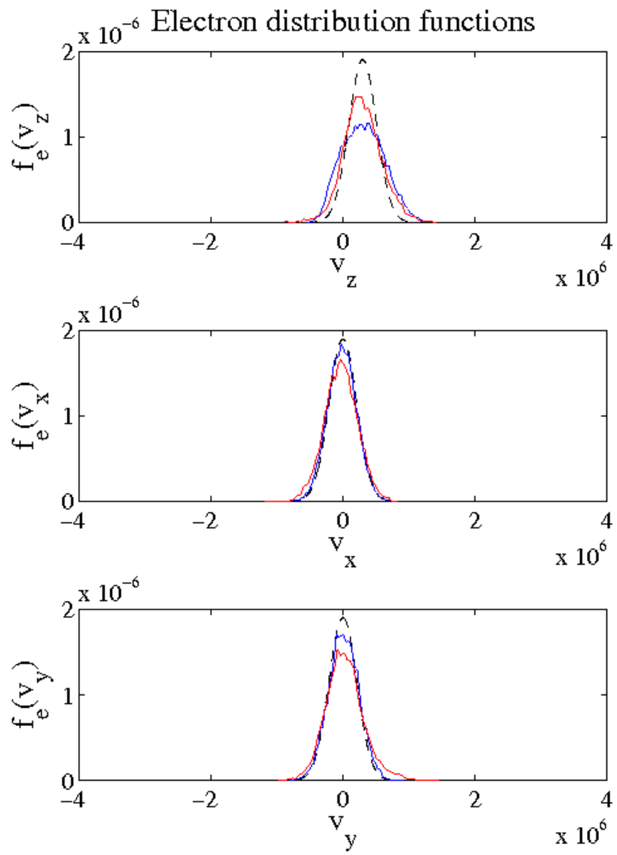

Electron distribution functions for $t = 0$ (dashed black line), $t = 240$ ns (blue line), and $t = 480$ ns (red line).

Simulation I

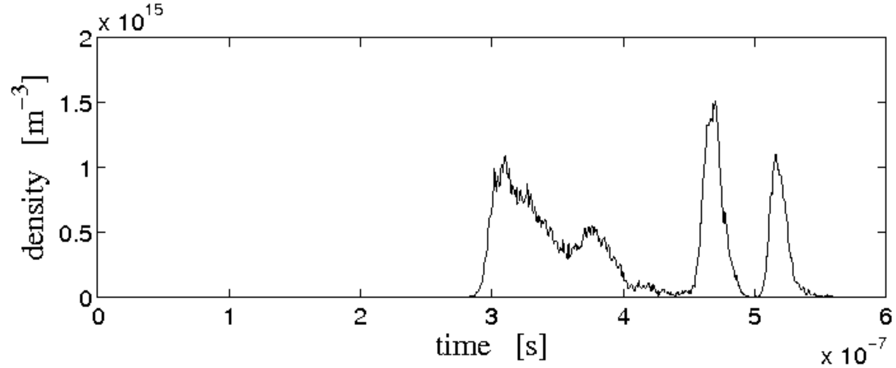

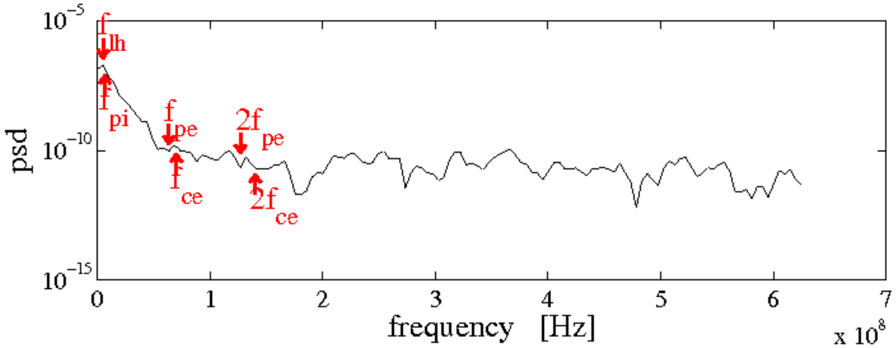

Density probe at $z = 0.21$ m.

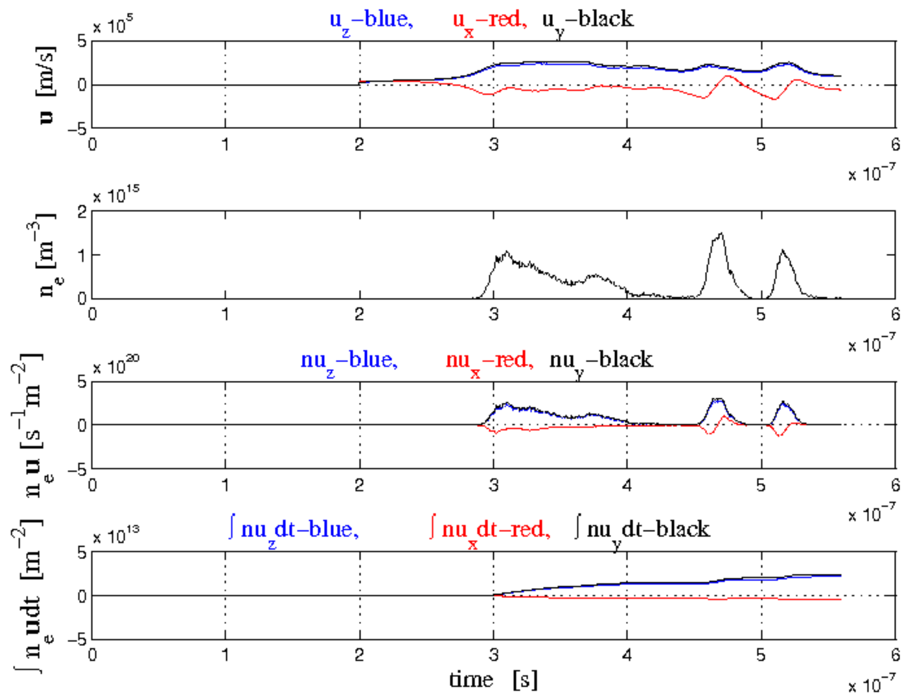

$\vec{E} \times \vec{B}$-drift at $z = 0.21$ m.

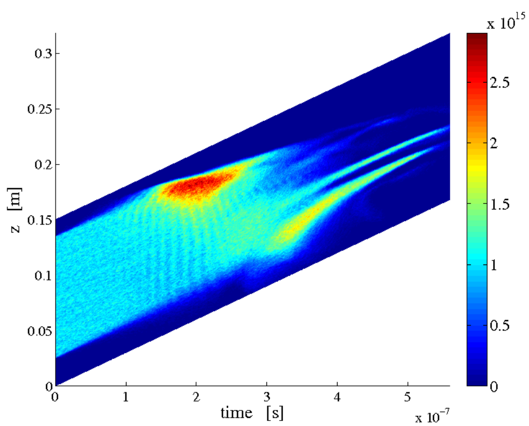

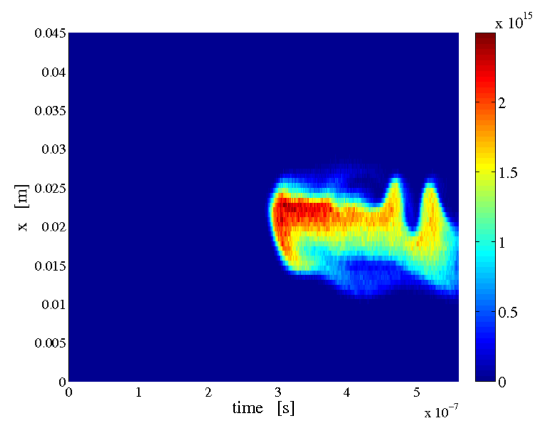

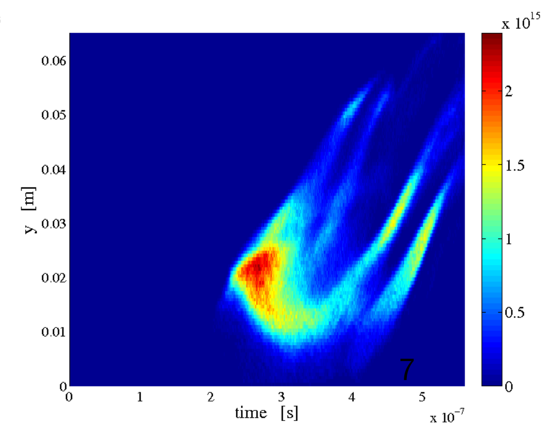

Simulation I

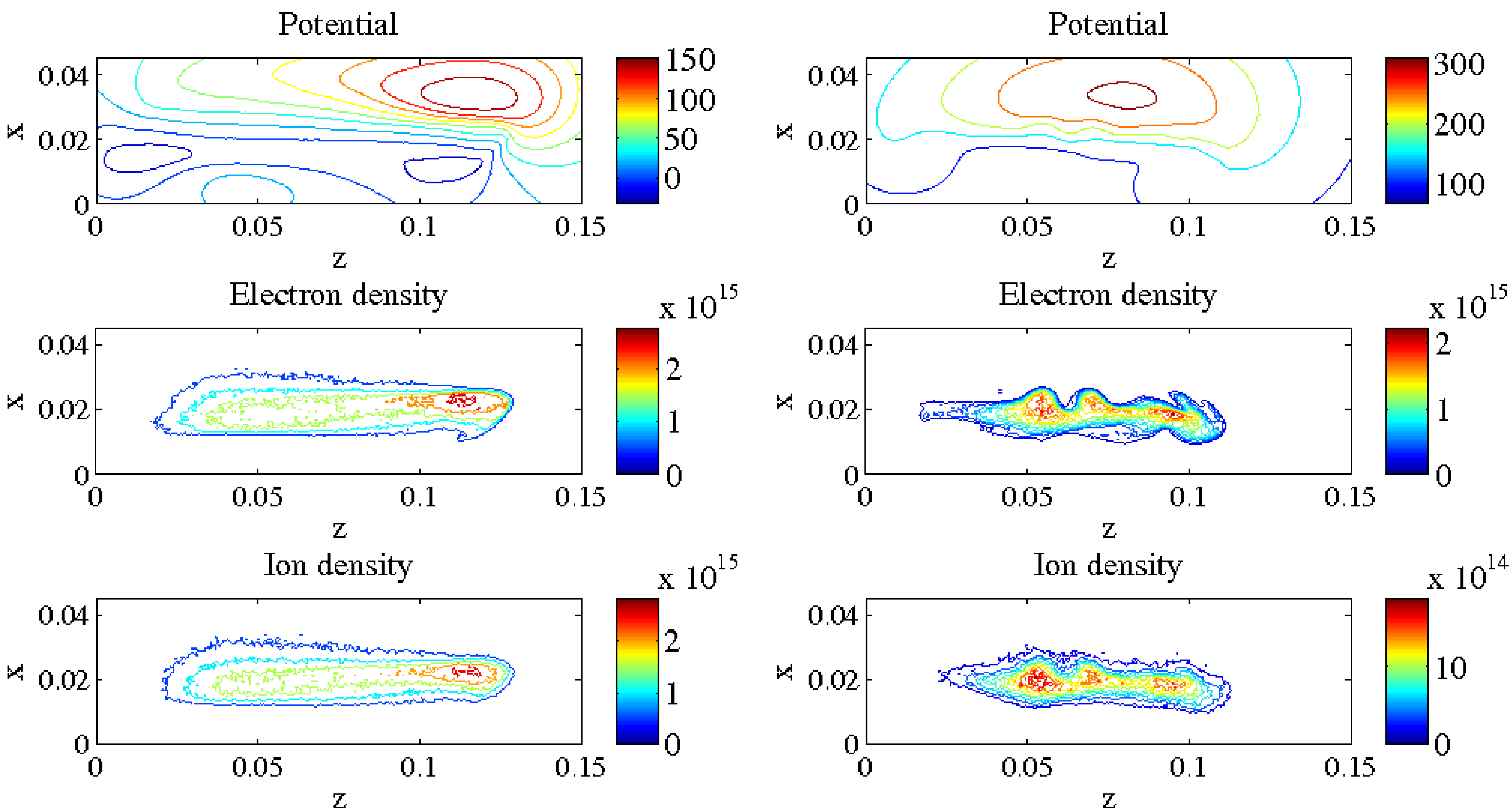

Potential and density contours at $t = 240$ ns and $t = 480$ ns.

Simulation II

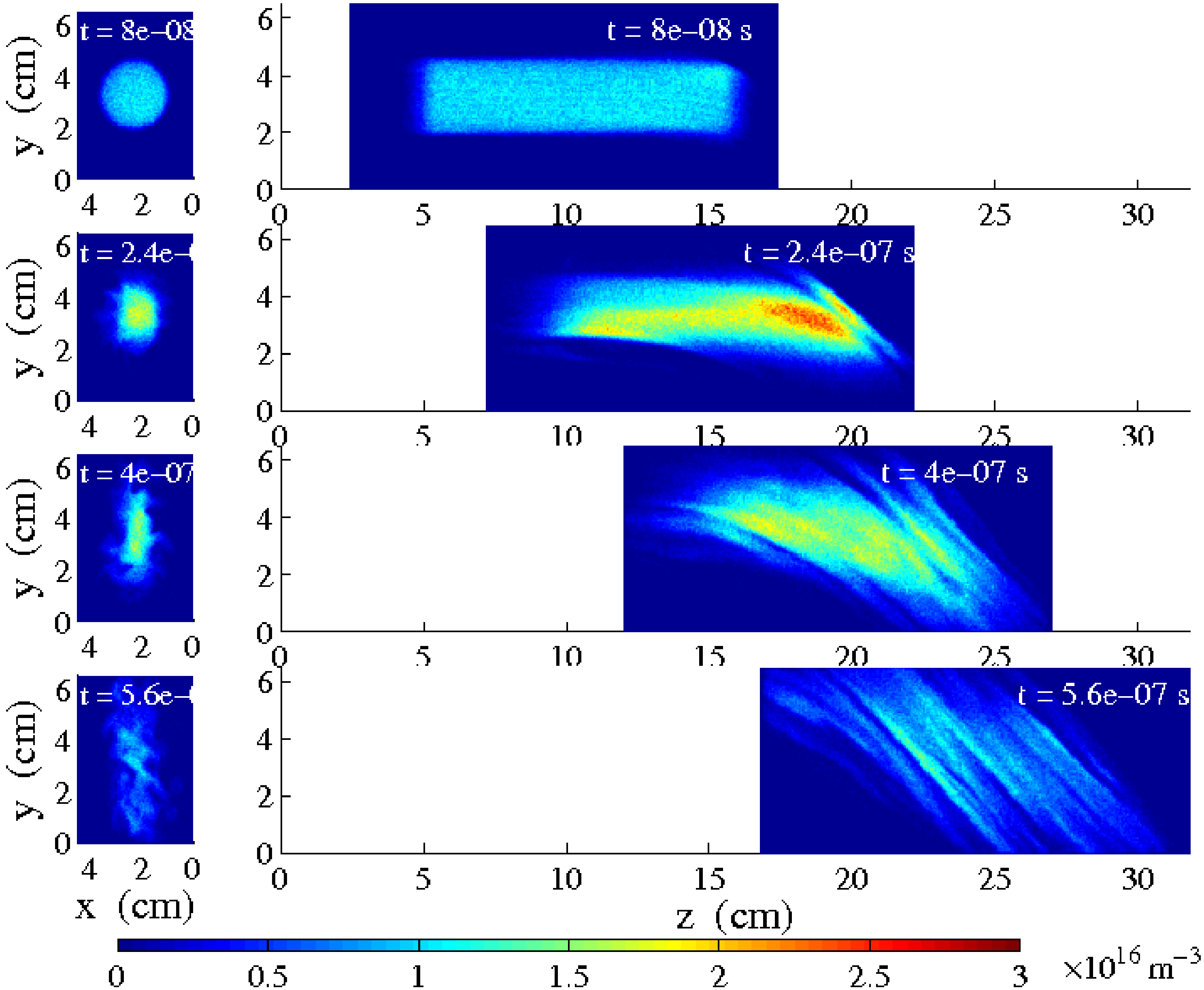

Electron density maps at different times.

Simulation II

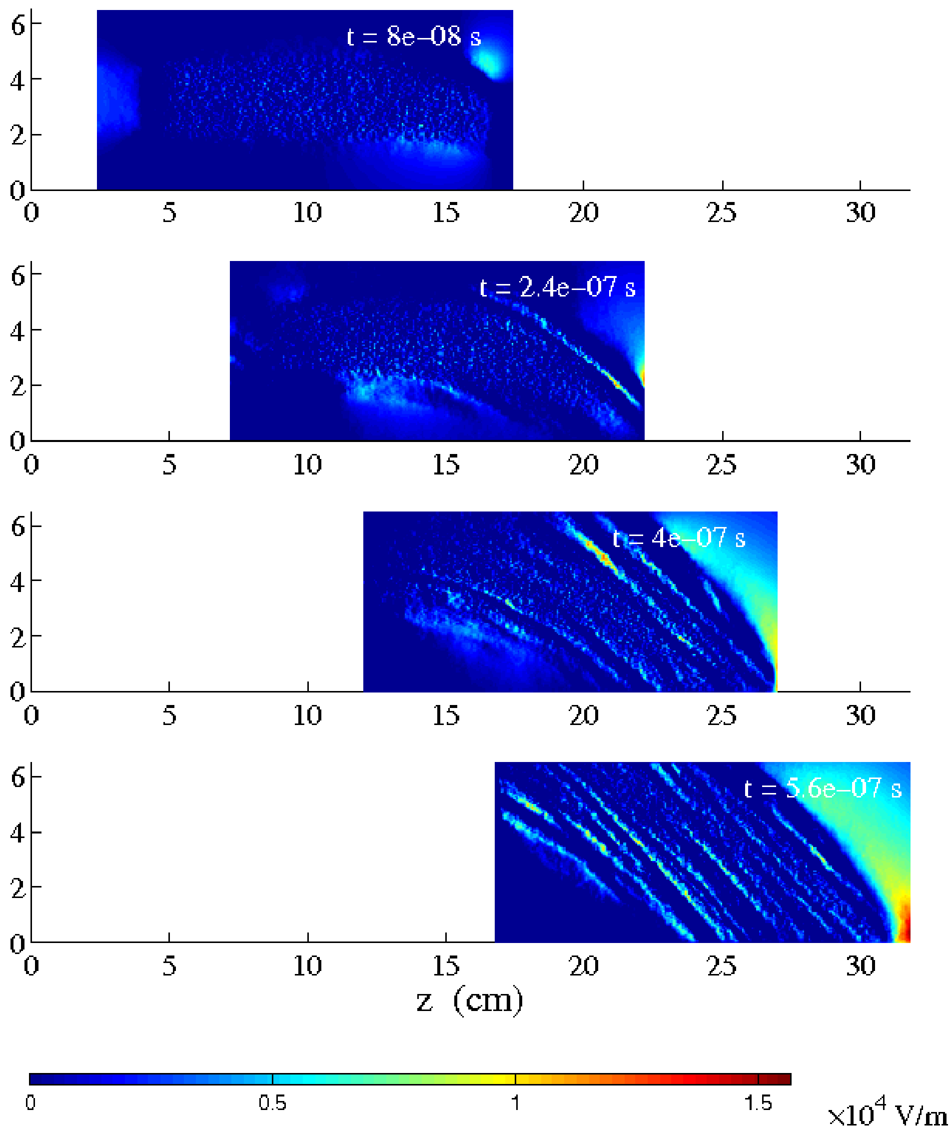

E_z maps at different times.

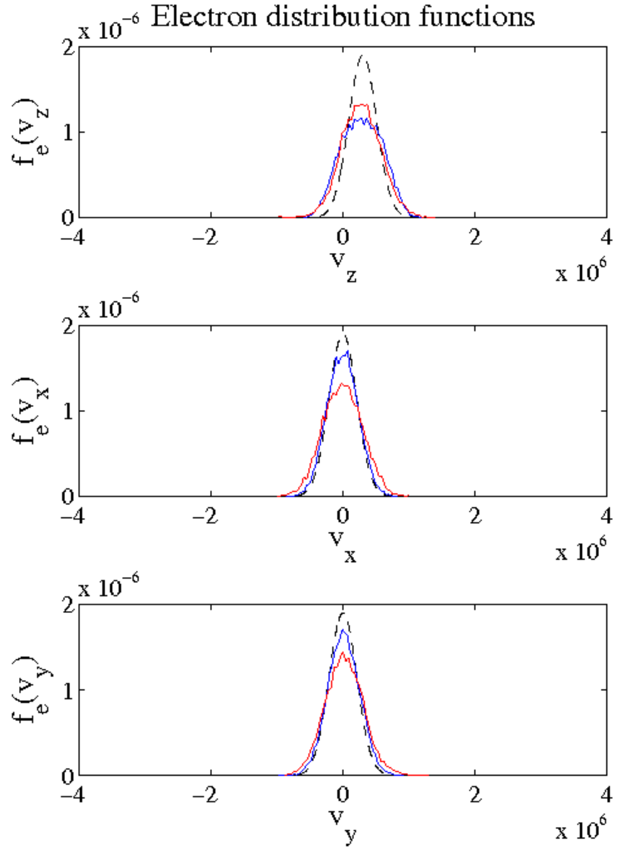

Electron distribution functions for $t = 0$ (dashed black line), $t = 240$ ns (blue line), and $t = 480$ ns (red line).

Simulation II

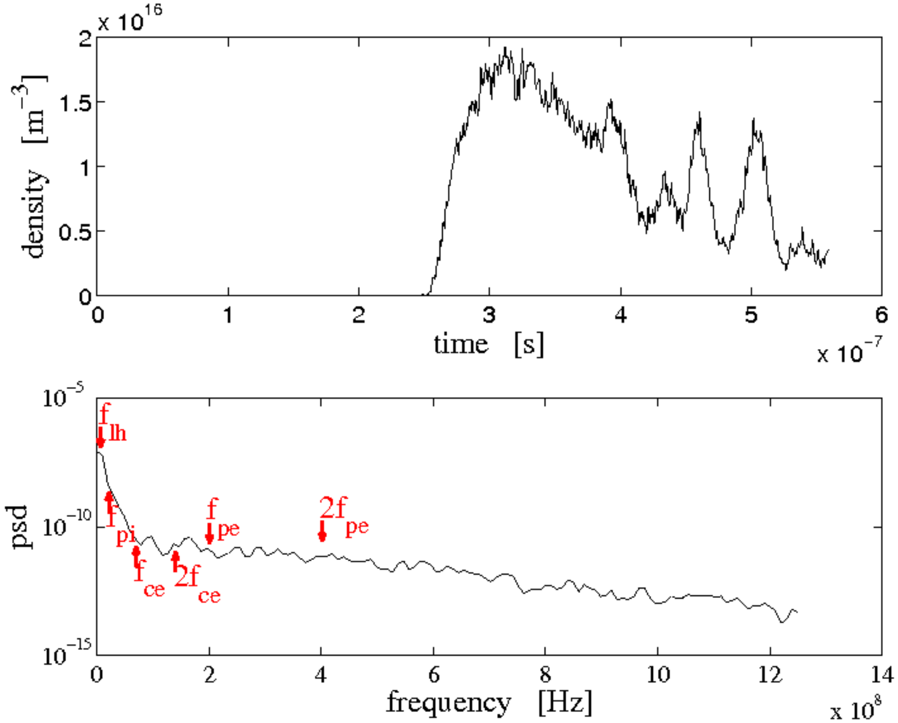

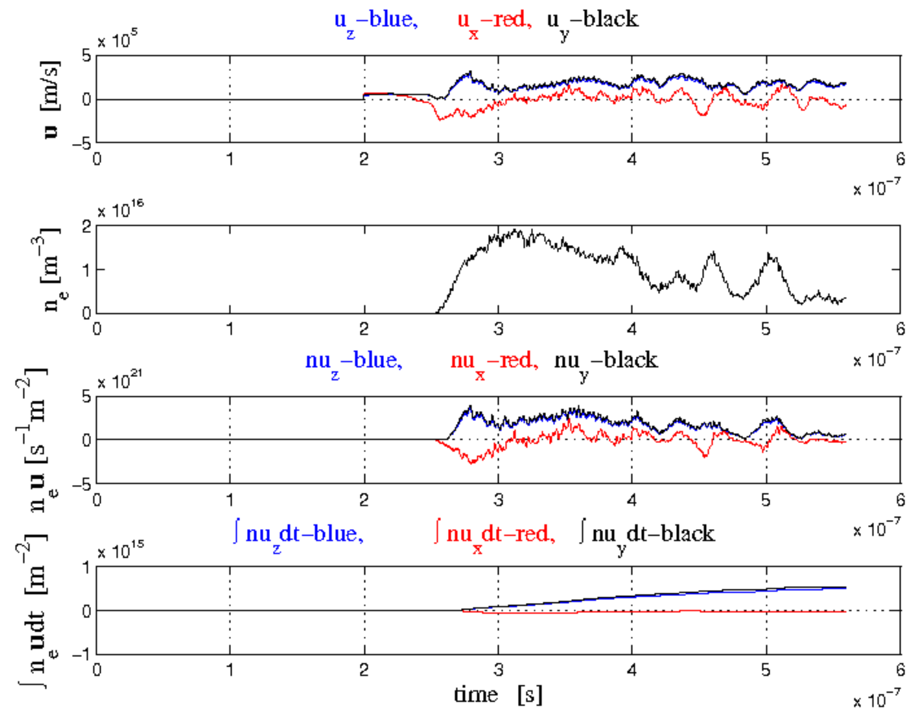

Density probe at $z = 0.21$ m.

$\vec{E} \times \vec{B}$-drift at $z = 0.16$ m.

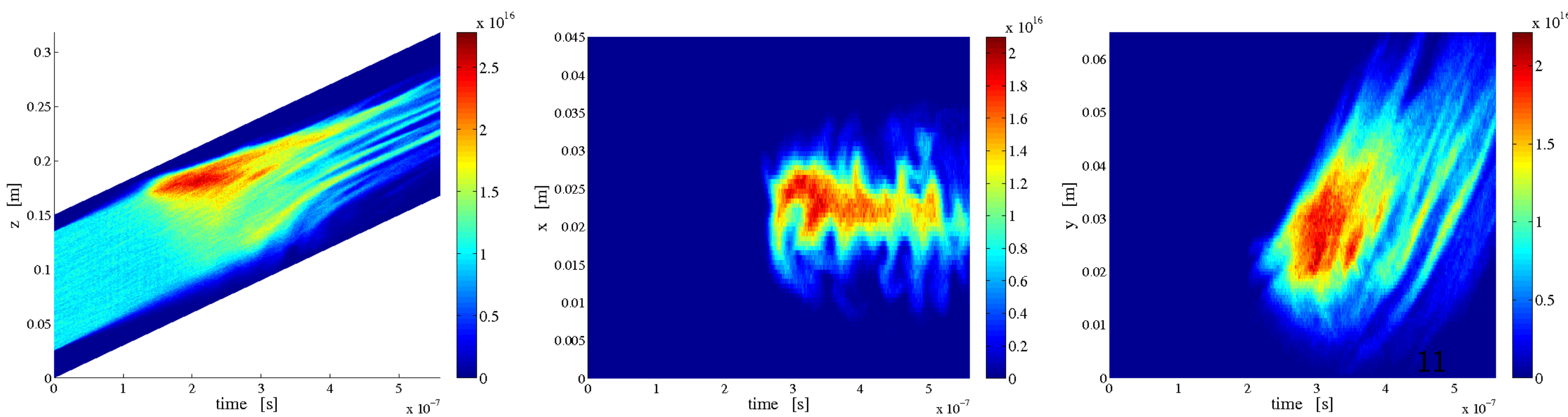

Simulation II

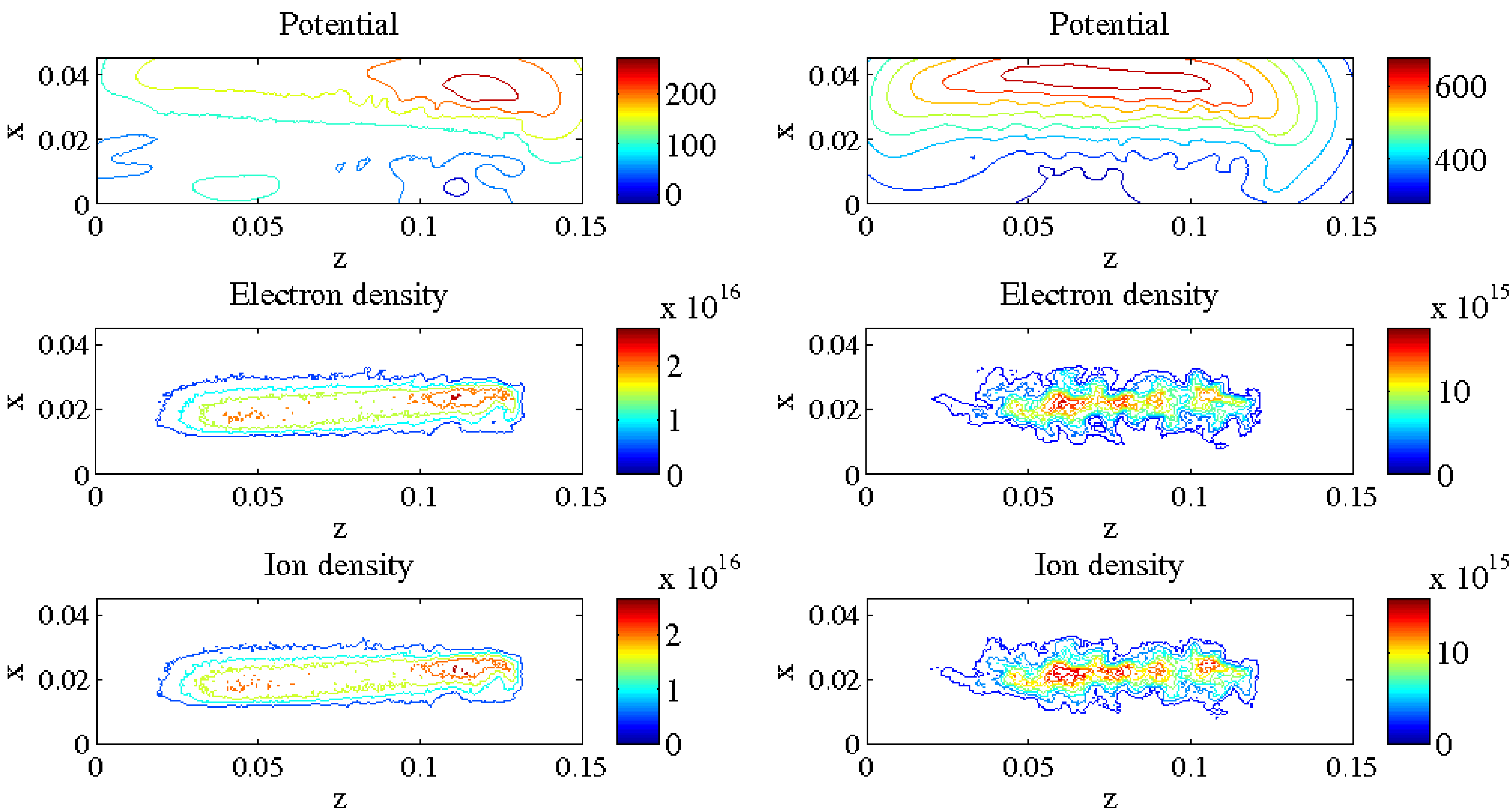

Potential and density contours at $t = 240$ ns and $t = 480$ ns.

and in Space

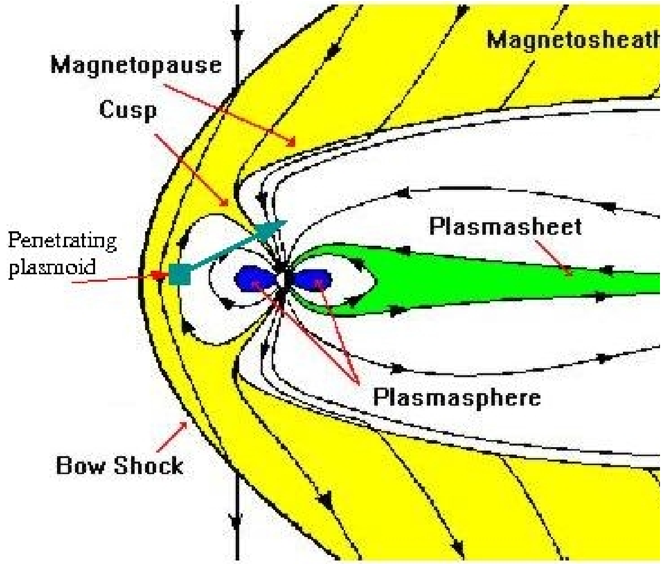

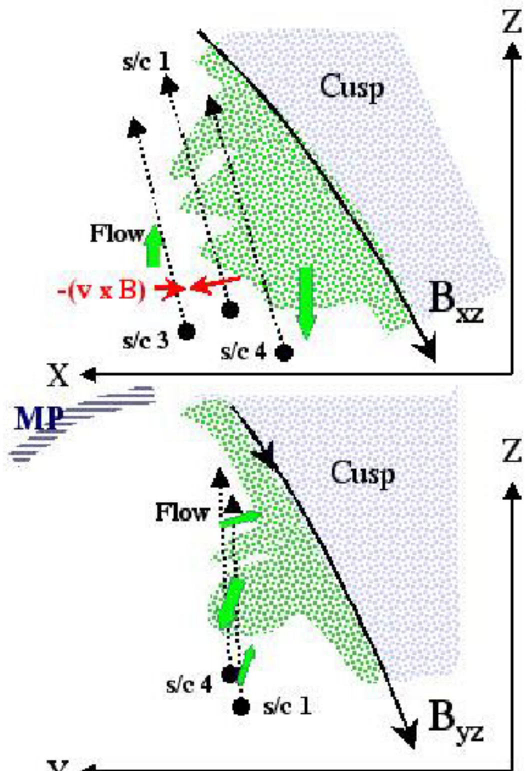

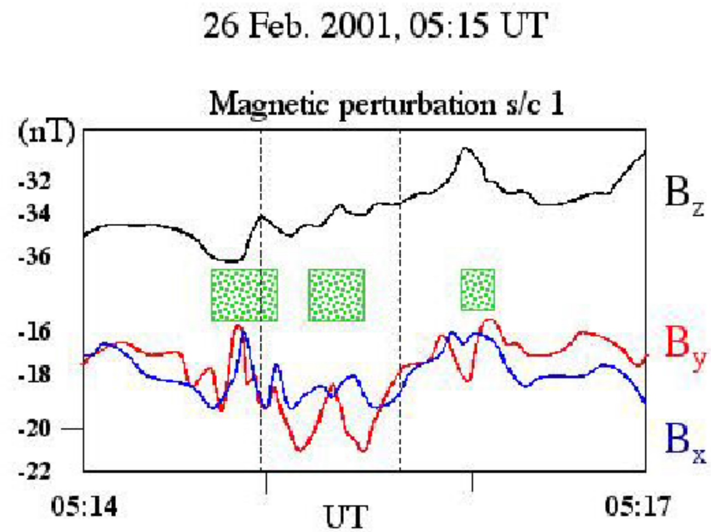

GSE	X (Re)	Y (Re)	Z (Re)
s/c 1	2.83	3.46	8.19
s/c 3	2.89	3.46	8.14
s/c 4	2.78	3.44	8.10

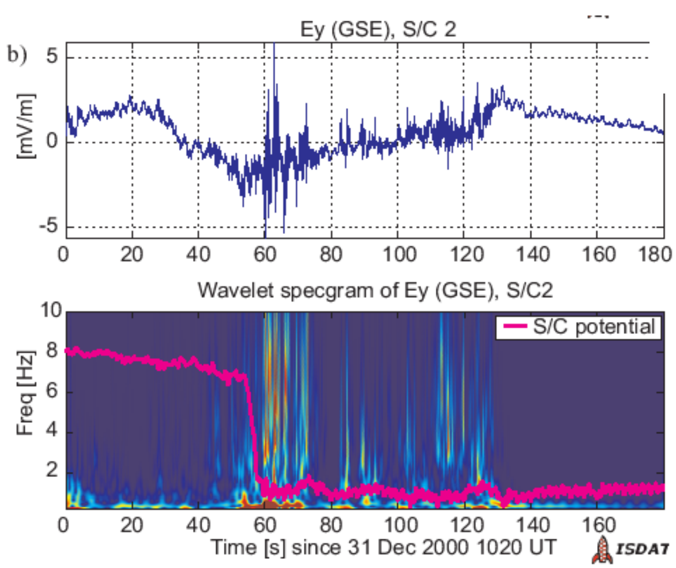

Above left: Schematic of the magnetosphere showing where penetration and convection take place. (Original picture from NASA)
Above right: Schematic by Lundin, et al., [8] showing penetrating plasmoids as observed by Cluster.
Left: Observation by the Cluster spacecraft of oscillations in the lower hybrid range on the inside of the magnetopause. (Picture from [9]).

Space

parameter	Magnetopause [9, 10]	sim. I	sim. II	exp.[2]
v_0/(km/s)	100–200	300	300	300
$B_\perp$/T	(10–30)$\cdot 10^{-9}$	0.05	0.05	0.015
n_0/m^{-3}	$\approx 2 \cdot 10^7$	10^{15}	10^{16}	10^{18}
W_K/W_E	(0.4–4)$\cdot 10^7$	76	756	$8 \cdot 10^5$
$\frac{1}{10}\frac{W_K}{W_E}\sqrt{\frac{m_e}{m_i}}$	(1–9)$\cdot 10^4$	0.79	7.9	$2 \cdot 10^3$
W_K/W_B	0.5–17	$8 \cdot 10^{-5}$	$8 \cdot 10^{-4}$	0.8
$\frac{w}{r_{\mathrm{gi}}}K\sqrt{\beta_{\mathrm{ith}}}$	?	$1.3 \cdot 10^{-3}$	$4.2 \cdot 10^{-3}$	0.1
f_{pe}	40 kHz	63 MHz	200 MHz	9 GHz
f_{ce}	(0.3–1.1) kHz	70 MHz	70 MHz	0.4 GHz
f_{pi}	0.9 kHz	7 MHz	20 MHz	0.2 GHz
f_{lh}	(7–26) Hz	5 MHz	7 MHz	10 MHz

Parameters at the magnetopause region [9], the two simulations presented here, and the experiments [2].

Upstream $\vec{B}$-direction

Lindberg [11] pointed out that the polarisation field builds up a potential which the ions must overcome. He found that this sets an upper limit to the width of the penetrating plasmoid:

$$w \leq \frac{1}{2}\frac{m_\mathrm{i} v_0}{\mathrm{e} B_y} = \frac{1}{2} r_\mathrm{gi}. \tag{1}$$

Here $B_y = B_\perp$ downstream and $B_y = 0$ upstream of the barrier. Since the solar wind is magnetised, this condition is modified at the magnetopause, where the upstream B_y may differ from zero. With the downstream magnetic field $\vec{B}_\mathrm{d} = B_{y\mathrm{d}}\hat{y}$, with the upstream field $\vec{B}_\mathrm{u} = B_{x\mathrm{u}}\hat{x} + B_{y\mathrm{u}}\hat{y} + B_{z\mathrm{u}}\hat{z}$, and with $\vec{v}_0 = v_0\hat{z}$, we have

$$\mathrm{e}w\left(-\vec{v}_0 \times \vec{B}_\mathrm{d} - \left(-\vec{v}_0 \times \vec{B}_\mathrm{u}\right)\right) \cdot \hat{x} = \mathrm{e}wv_0\left(B_{y\mathrm{d}} - B_{y\mathrm{u}}\right) \leq \frac{m_\mathrm{i} v_0^2}{2}. \tag{2}$$

From (2) we obtain the following plasmoid-width condition.

$$w \leq \frac{1}{2} r_\mathrm{gi} \frac{B_{y\mathrm{d}}}{B_{y\mathrm{d}} - B_{y\mathrm{u}}} \tag{3}$$

Conclusions

- We have presented three-dimensional electrostaic particle in cell simulations of plasma penetration of a magnetic barrier. We simulated two cases: simulation I with $n_0 = 1 \cdot 10^{15}\mathrm{m}^{-3}$, and simulation II with $n_0 = 1 \cdot 10^{16}\mathrm{m}^{-3}$.

- Waves in the lower-hybrid frequency range are observed.

- Accounting for the upstream magnetic field, Lindberg's [11] condition on plasmoid width becomes $w \leq \frac{1}{2} r_{\mathrm{gi}} \frac{B_{y\mathrm{d}}}{B_{y\mathrm{d}} - B_{y\mathrm{u}}}$.

- The plasmoid width, w, is a crucial quantity for the understanding of the penetration process.

- The search for penetrating plasma structures should emphasise cases in which the interplanetary magnetic field is oriented northward, as this configuration is less likely for reconnection.

References

[1] H. Gunell, T. Hurtig, M. Koepke, and N. Brenning, "Simulations of a plasmoid penetrating a magnetic barrier," *Plasma Physics and Controlled Fusion*, 2007. submitted.

[2] T. Hurtig, N. Brenning, and M. A. Raadu, "Three-dimensional electrostatic particle-in-cell simulation with open boundaries applied to a plasma beam entering a curved magnetic field," *Physics of Plasmas*, vol. 10, pp. 4291–4305, 2003.

[3] G. Schmidt, "Plasma motion across magnetic fields," *Physics of Fluids*, vol. 3, no. 6, pp. 961–965, 1960.

[4] W. Peter and N. Rostoker, "Theory of plasma injection into a magnetic field," *Physics of Fluids*, vol. 25, no. 4, pp. 730–735, 1982.

[5] H. Ishizuka and S. Robertson, "Propagation of an intense charge-neutralized ion beam transverse to a magnetic field," *Physics of Fluids*, vol. 25, no. 12, pp. 2353–2358, 1982.

[6] T. Hurtig, N. Brenning, and M. A. Raadu, "The role of high frequency oscillations in the penetration of plasma clouds across magnetic boundaries," *Physics of Plasmas*, vol. 12, p. 012308, 2005.

[7] N. Brenning, T. Hurtig, and M. A. Raadu, "Conditions for plasmoid penetration across abrupt magnetic barriers," *Physics of Plasmas*, vol. 12, p. 012309, 2005.

[8] R. Lundin, J.-A. Sauvaud, H. Rème, A. Balogh, I. Dandouras, J. M. Bosqued, C. Carlson, G. K. Parks, E. Möbius, L. M. Kistler, B. Klecker, E. Amata, V. Formisano, M. Dunlop, L. Eliasson, A. Korth, B. Lavraud, and M. McCarthy, "Evidence for impulsive solar wind plasma penetration through the dayside magnetopause," *Annales Geophysicae*, vol. 21, pp. 457–472, Feb. 2003.

[9] M. André, R. Behlke, J.-E. Wahlund, A. Vaivads, A.-I. Eriksson, A. Tjulin, T. D. Carozzi, C. Cully, G. Gustafsson, D. Sundkvist, Y. Khotyaintsev, N. Cornilleau-Wehrlin, L. Rezeau, M. Maksimovic, E. Lucek, A. Balogh, M. Dunlop, P.-A. Lindqvist, F. Mozer, A. Pedersen, and A. Fazakerley, "Multi-spacecraft observations of broadband waves near the lower hybrid frequency at the earthward edge of the magnetopause," *Annales Geophysicae*, vol. 19, pp. 1471–1481, 2001.

[10] D. Sundkvist, A. Retinò, A. Vaivads, and S. D. Bale, "Dissipation in turbulent plasma due to reconnection in thin current sheets," *Phys. Rev. Lett.*, vol. 99, p. 025004, 2007.

[11] L. Lindberg, "Plasma flow in a curved magnetic field," *Astrophysics and Space Science*, vol. 55, pp. 203–225, May 1978.